

https://dspace.org/

Electrospun nanofibrous scaffolds as a platform to reduce melanoma tumour growth recurrenceand promote postresection wound repair

N Goonoo; F Gimie; I Ait-Arsa; M Ziman; Samson Adeyemi ...

https://hdl.handle.net/10539/42691
WOS

Downloaded from a DSpace repository. https://dspace.org/

Biomaterials Advances 161 (2024) 213870

Contents lists available at ScienceDirect

Biomaterials Advances

journal homepage: www.journals.elsevier.com/materials-science-and-engineering-c

Electrospun nanofibrous scaffolds as a platform to reduce melanoma tumour growth, recurrence, and promote post-resection wound repair

Nowsheen Goonoo[a], Fanny Gimie[b], Imade Ait-Arsa[h], Melanie Ziman[C], Samson A. Adeyemi[d], Philemon Ubanako[0], Lindokuhle M. Ngema[0], Yahya E. Choonara[d], Archana Bhaw-Luximon[a,•]

• *Biomatmals, Dnl& Dtlive,y and Nanotechnology* Uni *Cmlr• for* lliomedka/ *and lliomaterials* Research, *Uniwrsiry of Mauritiw,* Redui *Mauritiw*
• *Anima/m,, Platefomte de recherche Cl'JIOI 2 rue Maxime Riviere, 97490 Sainte Clotilde, lle* De *La R.unionFranco*
< *School of M cal and Heald! Scitnces, Edid! Cowan Uni l Imiry, Perth, Awtralia*
d *WITS Advanced Drug Delivery Plalfomt,* Univmiry *of Wiuwatersrand, Johamtesburg, S-Oud! Africa*

ARTICLE INFO

Keywords.
Melanoma
Fucoidan
Nanotibers
Cancer Regenerative Med1cme

ABSTRACT

Wound healing following skin tumour surgery still remains a ma,or challenge. To address this issue, polysaccharide-loaded nanofibrous mats have been engineered as skin patches on the wound site to improve wound healing while simultaneously eliminating residual cancer cells which may cause cancer relapse. The marine derived polysaccharides kappa-carrageenan (KCG) and fucoidan (PUC) were blended with polydioxanone (PDX) nanofibers due to their inherent anti-cancer activity conferred by the sulphate groups as well as their immunomodulatory properties which can reduce inflammation resulting in accelerated wound healing. KCG and FUC were released sustainably from the blend nanofibcrs l'ia the Korsmeyer-Peppas kinetics. MTT assays, live/dead staining and SEM Images demonstrated the toxicity of KCG and FUC towards skin cancer MP 4 1 cells. In addition, MP 4l cells showed reduced metastatic potential when grown on KCG or FUC containing mats. Both KCG and FUC were non• cytotoxic to healthy L 929 fibroblast cells. *In vivo* studies on healthy Wistar rats confirmed the non-toxicity of the nanofibrous patches as well as their improved and scarless wound healing potential. *In vivo* studies on tumour xenograft model further showed a reduction of 7_15 % in tumour volume in only **4** days following application of the transdermal patch.

1. Introduction

Melanoma is known for its aggressiveness, metastatic nature and treatment resistance. Treatment usually depends on the tumour location, degree of progression and tumour size. Surgical resection remains the most commonly used and preferred treatment option. However, it is very difficult to remove the cancerous tissue completely and local tumour recurrence arising from residual cancer cells remains a major challenge. Chemotherapy, photothennal therapy and immunotherapy are often considered as adjuvant post-surgery treatment to decrease the risk of recurrence [l]. Poor healing of the surgical wound due to altered microenvironment caused by the tumour is a second challenge [2]. In addition, the wound is prone to bacterial infection which further delays the wound healing process and skin regeneration 13].

The healing/closure of these incisional wounds is heavily impaired due to a chronic inflammatory micro-environment after surgical tumour removal I**4**]. Manica et al. [4) showed that pro-inflammatory cytokines were elevated due to high extracellular ATP levels after tumour removaL In addition, cancer patients are usually given radiotherapy post-tumour removal which results in unintended injury to overlying skin and further contributes to poor wound healing (5). Recent studies have shown that there is a high degree of overlap between cell signaling in wound healing and cancer such that most anti-cancer treatments interfere with the wound healing process. For instance, inflammation, which is crucial in wound healing, is actually an important driver of cancer. Thus, the use of tissue engineering scaffolds as platfonns to prevent the proliferation of residual cancer cells through controlled therapy release while simultaneously promoting wound healing in cancer patients is an interesting avenue to pursue [61-

A number of studies have reported on the use of nanoscaffolds as drug delivery systems following the removal of solid tumours. Since melanoma grows superficially on skin, the scaffolds can be applied *via* the transdennal route on the tumour site post-tumour removal. Transdennal drug delivery systems offer improved drug bioavailability,

• Corresponding author.
E-mail address: a.luximon@uom.ac.mu (A. Bhaw Luximon).

hnps:t do1,org/10.1016,J.b,oadv-2024.213870
Received 13 February 2024; **RKeived** invised form 17 April 2024; Accepted 20 April 2024
Available online 28 April 2024
2772•9508/li:) 2024 ElseVJer **B.**V. All rights reserved.

improved drug solubility, better stability, and prolonged half-life [7]. Among the various melanoma drug delivery systems investigated, electrospun mats have been widely studied due to specific properties such as cost effectiveness, high specific surface area, high porosity, diverse composition, controllable and adjustable microstructures and ease of functionaliz.ation [11). However, only few studies have Investigated the use of scaffolds as both drug delivery vehicles and scaffold for skin repair [9,10).

Sulphated polysaccharides such as kappa carrageenan (KCG) and fucoidan (FlJC) obtained from red and brown seaweeds, respectively display excellent biological features including anti-oxidant, anti-inflammatory anti-coagulant, and irnmunomodulatory activities relevant for wound healing applications [11]. In addition, growing literature suggest that KCG and FUC also possess anti-cancer properties [12,131. The sulphate content as well as the position of sulphate group on sugar backbone influence the anti-cancer activity of the polysaccharides Cl•,JS]. Anti-cancer activity of KCG and FUC have been reported in several cell lines such as HeLa, HepG2, colorectal carcinoma, breast cancer, bladder cancer cells, liver cancer cells (16--21]. The anti-tumour activity ofKCG was related to the destabilization of the interaction of the GAG portion of the proteoglycans with ECM proteins, thereby eliminating the adhesion of cancer cells to matrices, which is necessary for metastasis (22). FUC induces apoptosls by both extrinsic (death receptors) and Intrinsic (mitochondrial) pathways. Interestingly, FUC does not result in apoptosis of healthy cells suggesting its safer use compared to conventional chemotherapy drugs [23].

To the best of our knowledge, there has been no reported study on the cytotoxic effect of sulphated polysaccharides KCG and FUC on human uveal melanoma cells and on their use in electrospun scaffolds to simultaneously prevent tumour recurrence and promote wound healing. We herewith report on the anti-cancer and anti-metastatic effect of KCG and FUC on human uveal melanoma cells and thelr non-cytotoxic effect and cytotoxic effects on healthy fibroblast and uveal melanoma cells respectively. *In vitro* studies were conducted under two different conditions; in particular, (I) using the electrospun mats as drug delivery vehicles only and (2) using the electrospun mats as cell support and as drug delivery vehicles (Scheme 1). *In vivo* studies on the scaffolds have also been conducted to confirm non-toxicity, accelerated wound healing and anti-cancer effects of the nanofibrous patches.

2. Materials and methods

PDX (Resomer X 2065, inherent viscosity 2.0, MW = 1.01 x 10^5 g/mol) was purchased from Evonik, Germany. 1,1,1,3,3,3-hexafluoroisopropanol (HFIP) purchased from Apollo Scientific (UK) was used as received. Kappa-carrageenan (KCG) with viscosity 0.3 % In H2O **and** chloroform (CHCl:J) **were usl!d** as received from Sigma-Aldrich. FUC **(Mw** • 80,000 g/mol) was purchasl!d from Lyphar Company, China.

2.1. ElectroSpinning

PDX/KCG and PDX/FUC were blended in the following ratios: 100/0, 90/10, 80/20, 70/30 *w/w%.* All polymer blend emulsions were stirred for 24 h before electrospinning. The solutions were prepared as described before [24]. Electrospinning was carried out using an electrospinning machine purchased from lnovenso Company (Turkey) (bottom-up NE300 Laboratory scale electrospinner). The electrospun fibers were collected as non-woven fiber mats on a static grounded aluminium target. After electrospinning, the scaffolds were removed from the collecting target and storl!d in a desiccation chamber until further analysis.

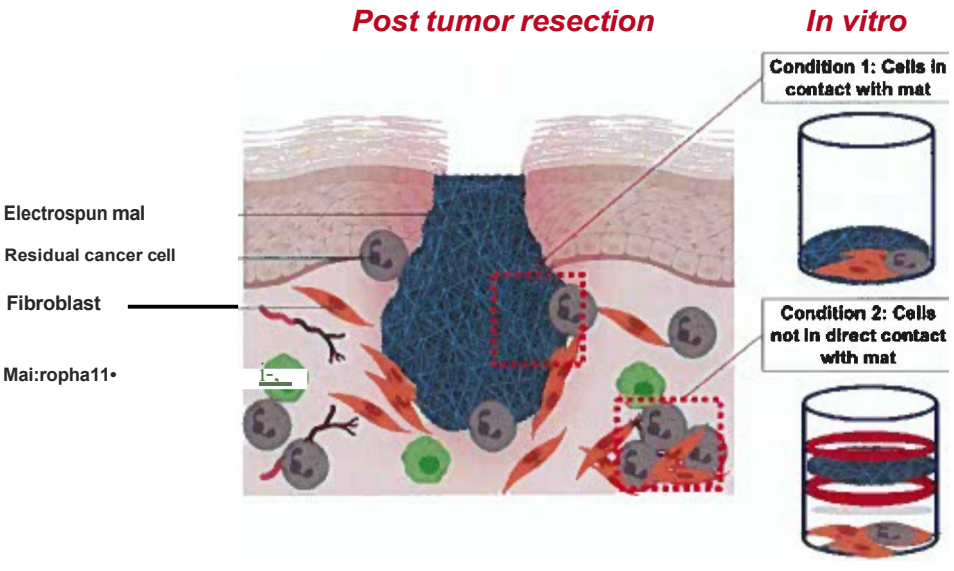
2.2. Fabrication of polymer films

PDX/KCG and PDX/FUC 80/20 films weres fabricated by preparing a 75 mg/ml solution. For PDX/KCG, a mixture of HFIP/CHCl3 was used in ratio 8/2 *v/v.*The KCG was dissolved first in CHC13followed by addition in a solution of PDX in HFIP. The mixture was stirred at 300 rpm for 5 h before casting in a silicone mould. PDX/FUC on the other hand was prepared by dissolving both polymers in HFIP. The mixture was stirred at 300 rpm for 5 h before casting In a silicone mould. The polymer films **were** allowed to dry for 48 h at room temperature until further use.

3. Experimental details

3.1. Choroctemation of electrospun mats

SEM images were acquired using a Tescan Vega 3 I.MU microscope (CBBR, Mauritius) with accelerating voltage of 30 kV'. Samples were prepared for SEM as described before [25). A Universal lnstron Tester 3344 (Instron, USA) was used to measure the tensile properties of the electrospun mats at 25 •**C.** The electrospun mats cut in rectangular



Scheme 1. Tumour resection area depicting residual cancer cells and healthy cells (1} in contact and (2) not In direct contact with the nanoscaffolds

shapes (4 x I cm^2) were clamped with gauge length set at 1 cm and strained at a rate of 10 mm/min using a load cell of 100 N.

3.2. Polysacchanae release from e/ectrosplUI mats

In-vitro drug release studies were carried out using electrospun POX/polysaccharide mats in weight varying ratios of KCG and FUC. Electrospun nanofibers of weighed amount was placed in 3 ml PBS (pH 7.4), at a temperature of 37 •C in an incubator. At regular intervals, I ml of aliquot was removed and replaced with the same quantity of the buffer. The amount of released polysaccharide was determined by UV visible spectrophotometer at 280 and 204 nm for KCG and FUC respectively using standard calibration curves.

Different mathematical models were used to determine the polysaccharide release mechanism. The release profiles were tried to fit to zero order, first order, Higuchi and Korsmeyer-Peppas kinetic models (Eqs. (1)-(4}) [26,27].

Zero order model : $M, = kt + M,$ (1)

First order model : $Mo = Mt'$ (2)

Hi.,uchi mtx!cl • $M,$ ktu (3)

Skell survival $\frac{1111mher\ of\ cell.<\ ma\ give11\ well\ al\ a\ given\ polv.<acc/1artde\ cm1ce111ra11m1}{mm1her\ of\ cell.f\ lll\ the\ ah.<em:e\ of\ pnly.<accharrde.f\ (TCPS)} \times ICJO$ (5)

Korsmeyer - Peppas mtx!cl : $\frac{M,}{M.,} = kt^{n}$ (4)

where **M,** is the amount of polysaccharide released at time t, Mo is the initial amount of polysaccharide in the blend mat, 1 is the fraction of released polysaccharide, k is the rate constant and n is the diffusion exponent which gives indication of the drug release mechanism.

3.3. H_2O_2 radical scavenging activity

The scavenging activity for hydrogen peroxide was measured according to the modified method of Ruch et al. **(28).** Different concentrations ofKCG and FUC aqueous solutions (0.3 ml) were added to 0.9 ml of PBS and 1.8 ml of H_20_2 solution (40 mM) In phosphate buffer {50 mM, pH 7.4), and the reaction mixture was Incubated at 25 •C for 10 min. The unreacted H_20_2 was determined by measuring the absorbance of their action mixture at 230 nm with respect to the blank solution. 1 mg/ml ascorbic acid was used as the positive control.

The percentage of hydrogen peroxide inhibition was calculated as follows:

'¼.[lhOzl inhibition= ((Ao-A1)/Ao)JOO

where Ao was the absorbance of the control, and A_1 was the absorbance of the sample.

3.4. Culture of MP 41 human uveal melanoma cells, L 929 mouse fibroblasts, murine RAW 264.7 macrophage cells

L 929 mouse fibroblasts (ECACC cenified) were bought from Sigma-Aldrich and RAW 264.7 macrophages were purchased from ATCC. The uveal melanoma cell line, MP41 was kindly supplied by Prof Melanie Ziman.

L 929 fibroblasts, and RAW 264.7 macrophages cells were cultured at standard conditions (37 •C, 5 % CO_2) as reponed earlier (29). Human uveal melanoma MP41 cells were cultured in RPMI-1640 supplemented with 20 % Fetal Bovine Serum (FBS), 2 mM L•glutamlne, sodium pyruvate and 1 % penicillin/streptomycin at 37 •Cand 5 % CO_2. Prior to cell seeding on electrospun mats, they were all disinfected by immersion in 70 % ethanol followed by 3 consecutive phosphate buffer solution (PBS} washings. Cells were imaged using Evos® FL Imaging microscope.

3.5. Dehydration of electrosplUI scaffolds for SEM analysis

Cell-seeded scaffolds were fixed for SEM analysis by immersion In 3 % (v/v) glutaraldehyde solution for 30 min followed by dehydration with 30 %, 50 %, 70 %, 90 % and 100 % ethanol solutions and washings with a 1/1. v/v mixture of 100 % ethanol/hexamethyldlsilazane (HMDS) and finally pure HMDS.

3.6. MIT Assay (% cell survival)

The MTI assay was conducted after different time intervals (1, 3 and 7 days) as reponed earlier (29) and absorbance values were measured at a wavelength of 570 nm using a Thermo Scientific Varioskan LUX Multimode Microplate Reader. The% cell survival was calculated using Eq. (5).

3.7. ELISA IL 6 and TNF-a assays

Mouse RAW 264.7 macrophages were seeded on scaffolds in a 96 well-plate at a cell density of 2.0 x I 0^4 cells/well. After 24 h culture, an ELISA kit (Invitrogen and Sigma-Aldrich) was used to measure the level of IL-6 and TNF-a respectively in the cell culture supernatant according to the manufacturer's instructions.

3.8. Live and dead staining

Triplicates of each blend mat were disinfected (30 min ethanol followed by three 10 min PBS washes) and transferred to 96-well plates and seeded with 20 000 cells/well. Cell viability was assessed after 24 h *via* live dead assay whereby cells were stained with FDA (5 mg/ml, Fluorescein diacetate; Sigma-Aldrich) and PI (2 mg/ml, Propidium Iodide; Carl Roth), respectively. Fluorescence microscopy images of live (green) and dead (red) cells were then acquired with an EVOS® FL Imaging microscope fluorescence microscope.

3.9. Cell staining and fluorescence microscopy analysis

Cells were stained using DAPI (for the nucleus) and Phalloidin-Alexa 488 (for actin). Briefly, the cell seeded scaffolds were washed with PBS, fixed with paraformaldehyde (4 % in PBS, 30 min; VWR), permeabilized with Triton X-100 (0.2 % in PBS, 10 min; VWR), and washed with PBS (3 times) at room temperature. Samples were incubated in a solution of Alexa Fluor™488 Phalloidin for 30 min (300 U/ml in I % **BSA;** Invitrogen, Llfe Technologies) as well as DAPI staining solution (Sigma-Aldrich) for 15 min. Samples were mounted with Ibidi mounting medium (Germany) on cover glass slides and attached to microscope slides. Images were then acquired with an EVOS® FL Imaging microscope fluorescence microscope.

3. IO. Analysis of RAW 264.7 cell morphology

Fluorescence images of cells were acquired and using Cell Profiler (Broad Institute, 2021), the cell area, nucleus area, cytoskeleton to nucleus area and actin edge intensity of each cell were quantified.

3.11. Wound scratch assay

The L 929 fibroblast and uveal melanoma MP 41 cells were cultured at a density of 4 x 10^4 cells/well in 48-well cell culture plate (Coming Inc., NY, USA) and incubated at 37 •C with 5 % CO_2 for 24 h. After the cells have reached confluency, the cell monolayer was scraped with a 200 µl pipette tip to create a fixed-width linear gap between the cells. After washing with PBS to remove non-adherent cells, different concentrations of KCG and FUC were added to the wells. After 24 h, optical Images of the migrated cells were taken using EVOS® FL Imaging microscope. The % coverage of cells ln the wounded area was quantified uslng CellProfiler's wound healing pipeline.

3.12. In Vivo Srudies

3.12.1. In vivo biocompatibility

In vivo biocompatibility studies were carried out as previously described under approval by the Ethical Committee of Reunion Island, APAFIS#l6368_ 2018052311219125_v3 [29]. Briefly electrospun fiber mats were subcutaneously implanted Into 9-week-old, male and female Wlstar rats (Janvier Labs, Saint Berthevin, France). Electrospun scaffolds (1.0 x 0.5 cm^2) were soaked in 70 % ethanol overnight. Ethanol was allowed to evaporate on the next day in a sterile cell culture hood and the dry scaffolds were rinsed three times with PBS for 5 min each and finally few drops of normal saline was added to the scaffolds prior to implantation.

The rats were anesthetized using isoflurane (lsoflo 100 "-, Zoetis,) throughout the surgery. The dorsal region of the rats was shaved, and disinfected with 70 % ethanol followed by betadine solution. The disinfection procedure was repeated 3 times. Buprenorphine (0.05 mg/**kg)** was then injected subcutaneously. Four slits (each 1 cm long) at equal distances (2 cm) from the spine **were** cut through the skin using a sterile scalpel blade so that subcutaneous pockets were created. Three layers of each scaffolds (average overall thickness 1 µm) were then inserted into the pockets using a pair of micro-dissecting forceps. The skin was sutured with intradermal suture (PGLA 4/0 suture) to close the pockets. The area was disinfected with betadine solution and the rats were allowed to recover from anesthesia. Males and females were housed in separate cages. Post-op verification was made every day to check for evidence of wound complications, such as redness, infection, seroma, abscess, hematoma, or skin dehiscence. After 2 weeks, the scaffolds were removed and fixed for SEM analysis. Furthermore, tissue sections were removed from all the rats and stained using Masson·s Trichrome. The scaffolds are labelled as follows: upper layer, middle layer and lower layer. Afterwards, the rats were euthanized with an intraperitoneal injection ofpentobarbital (100 mg/kg).

3.12.2. In vivo wound healing studies

In vivo wound healing studies on Wistar rats were carried out as described in details in our previous publication under approval by the Ethical Committee of Reunion Island, APAFIS#2019070515468996_Vl [29].

3.12.3. In vivo anti-cancer srudies

Female athymic MFI-nu/nu nude mice (4-6 weeks old; 18-22 g) were acquired with approval from the University of the Witwatersrand's Animal Research Screening Committee, ethical clearance number 2020/11/01/B. The mice were housed in cages at a temperature of 25•C with continuous aeration, fed ad libirum and monitored.

To Induce tumour formation, the mice were anesthetized with isoflurane and then injected on their right flank with 100 µI suspension containing 1 x 10^6 A 549 lung adenocarcinoma cells in sterile phosphate-buffered saline (PB.5). The control mouse was injected with 100 µl of sterile PBS. They were transferred to their respective cages for recovery and maintained for 28 days until the tumour reached around 15 mm diameter. The nanofibrous mats were then placed over the tumours for 4 days. The mats were attached onto the surface of the solid tumour and held in place using tegaderm.

After 4 days, the mice were euthanized using chlorofonn. Tumour diameters were measured using a digital calliper, and the tumour volume was calculated using Eq. (6) before and after treatment with the nanoflbrous patch. The tumours as well as the main organs (liver, spleen, and lung), were surgically excised, temporarily stored at •80 •C and subsequently sent for further histological (H & E) analysis.

$$V = w^2 \cdot l/2 \quad (6)$$

where w: width and I: length.

3.13. Statistical analysis

The data are presented as arithmetic mean± standard error of mean. Statistical analyses were done with the one-way or two-way analysis of variance CANOVA) test (OriginPro 8.5, Origin lab Corporation, USA). A value of $p < 0.05$ was considered statistically significant.

4. Results and discussion

KCG and FUC were first assessed to detennine their cytotoxicity and effects on mouse fibroblasts (L 929) and macrophages (RAW 264.7) cell lines which are involved in the proliferative and inflammatory phases of wound healing respectively. MP 41 was used as a model melanoma cell line to investigate the influence of the sulphated polysaccharides KCG and FlJC on cancer cells.

4.1. Cytotoxicity of KCG and FUC on different cell lines: MP 41, L 929 and RAW 264.7

Different concentrations of the polysaccharides in cell culture media were tested on both cancer and healthy cell lines to determine the minimum concentration required to induce cytotoxicity. The concentration of KCG was varied from O to I mg/ml while that of FUC ranged between O and 100 µg/ml. The % cell survival of the human uveal melanoma MP 41 cells, murine fibroblasts L 929 and murine macrophages RAW 264.7 were quantified at different time intervals namely after1 and 3 days (Flg. 1). Increasing the concentrations of KCG and FlJC led to decreased cell survival after 3 days. 1n addition, 100 µg/ml FUC was more cytotoxic to MP 41 cells compared to 1 mg/ml KCG. KCG and rue displayed much lower cytotoxicity to murine fibroblasts L 929 compared to MP 41.100 µg/ml FUC led to approximately 75.0 :I: 10.3 % L929 cell viability compared to 56.5 ± 7.2 % MP 41 survival after 3 days. In contrast, the polysaccharides showed high cytotoxicity against murine macrophage RAW 264.7 cells. More specifically, KCG and FUC concentrations ranging between 0.0625 and I mg/ml and 6.25-100 µg/ml respectively resulted In about 70 ,. RAW 264.7 cell viability following 3 days culture. In general, the polysaccharides reduced cell viability in the following order: MP 41 < RAW 264.7 < L 929.

4.2. Cell migration in cancer and wound healing

While being cytotoxic to cancer cells, it is important that the polysaccharides do not cause significant healthy cell death in the tumour resection area as this would delay wound closure. One of the most important processes in wound healing is fibroblast migration. Following

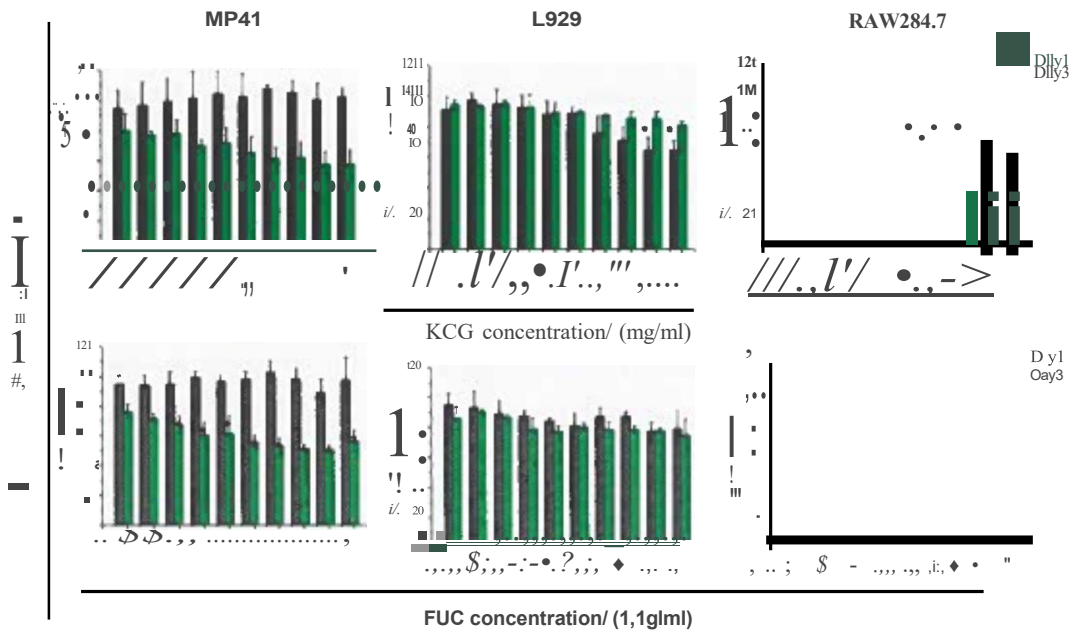


Fig. 1. % cell survival of MP41, L929 and Raw 264.7 cells following addition of KCG and FUC of varying concentrations. All measured values of KCG and FUC were compared with those of the lowest polysaccharide concentration: *$p < 0.05$; **$p < 0.0001$ and (ns) not significant wherever not indicated.

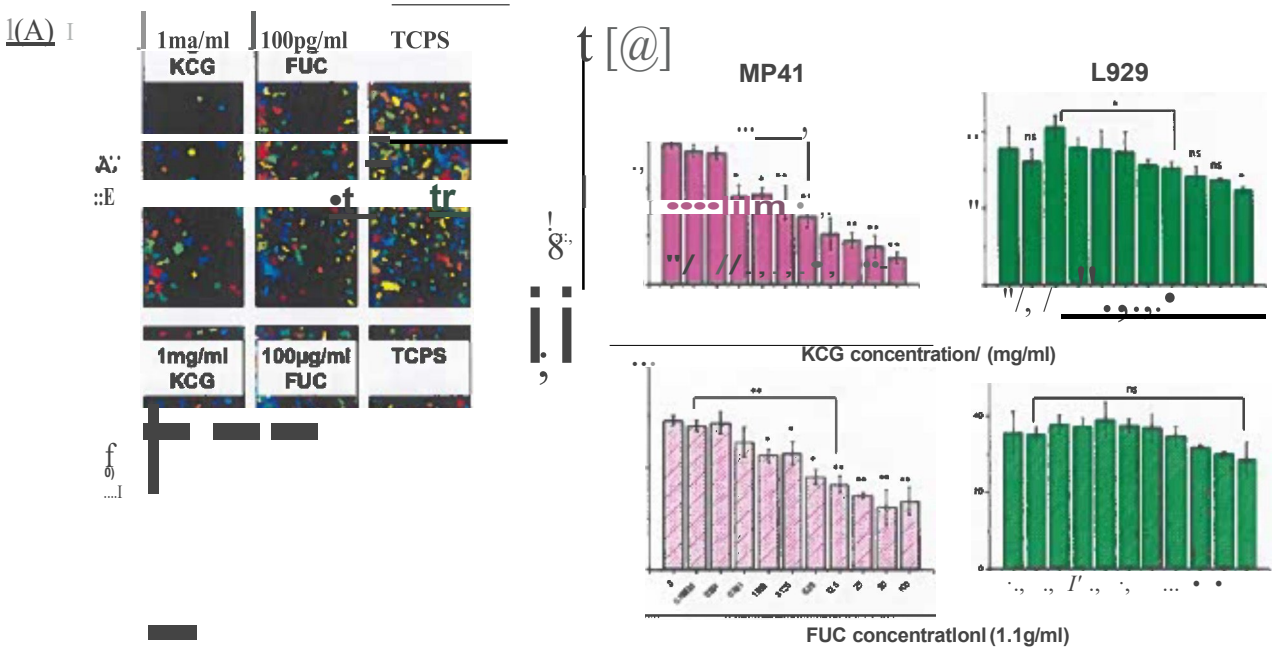


Fig. 2. (A) Processed image from Cell Profiler depicting cells migrated within the wound area (TCPS stands for tissue culture polystyrene) and (B) Graphs displaying the variation of%wound closure for various concentrations of KCG and FUC for MP 41 and L 929 cell lines. All measured values of KCG and FUC were compared with TCPS: *$p < 0.05$; ••$p < 0.0001$ and (ns) not significant wherever not indicated.

an injury, a blood dot is fonned and fibroblasts start migrating into the wounded area, biochemically degrading the fibrin clot and replacing the blood clot with collagen. Poor fibroblast migration leads to delayed or poor healing (30]. We therefore assessed the effect of KCG and FUC on healthy murine fibroblast 1929 cell migration.

The wound scratch assay was used to detennine the influence of KCG and FUC on cell migration using L 929 and **MP** 41. The scratch area is herewith referred to the 'wound' and the'%wound closure' refers to the % area covered by cells in the wound. From Fig. 2, it can be noted that both polysaccharides prevented MP 41 cell migration in a dose dependent manner. 1 mg/ml KCG inhibited MP 41 cell migration by six fold while the highest concentration of FUC *Le.* 100 µg/m1 almost inhibited cell migration by half compared to when the cells did not receive any treatment. However, FUC did not significantly inhibit fibroblast cell migration after 24 h which suggested that it would not drastically impede wound healing. On the other hand, 1 mg/ml KCG slightly decreased the % fibroblast cell migration and may result in delayed wound healing.

4.3. Inftammarory response of KCG and FUC on murine macrophages

The influence of the pure polysaccharides at different concentrations on the attachment, spreading, and phenotype of murine RAW 264.7 macrophages was investigated. The maximum concentration of KCG and FUC used were 1 mg/ml and 100 µg/ml respectively. The macrophages adopted a similar morphology to those cultured on TCPS when treated with varying concentrations of KCG. However, at high concentration, more floating and dead cells were noted. On days 2 and 3, the cells maintained the same round morphology but the number of unattached and dead cells increased as can be noted from the optical images in Fig. SlA. On the other hand, macrophage cells treated with FUC adopted spindle shape morphology (Fig. S1B). At high FUC concentration, a high proportion of spindle shaped cells were noted with very few round cells. As the concentration of FllC decreased, more round cells could be observed (Figs. 3 and S1B). With increasing time (day 3), more floating dead cells were observed at high FUC concentrations. Jnterestingly, the cytoskeleton area of RAW 264.7 cells increased with increasing FUC concentration *i.e.* more cell spreading was observed (Fig. **4B**). Th.is was in line with the ratio of cytoskeleton to nucleus area (Fig. 4D). In contrast, no drastic change was noted for cell area and cytoskeleton to nucleus ratio following treatment of RAW 264.7 cells with KCG (Fig. 4A and C). According to Rostam et al. [3l) M2 macrophages display much larger cell area compared to MO or Ml phenotypes and adopt more elongated structures [32). This suggests that FUC treatment promotes a phenotype change towards M2 i.e. the pro-healing and anti-inflammatory phenotype. Studies have shown that the pro-inflammatory cytokine IL-6 was responsible for promoting polarization of macrophages towards the M2 phenotype *via* NF-rll and JAK/STAT3 pathways. Interleukin (IL)-6 plays an important role in the inflammation phase and is responsible for the timely resolution of wound healing (33). ELISA assay was used to quantify the level of the pro-inflammatory cytokine IL-6 (Table 1). The highest concentration of KCG led to insignificant production of IL-6 in macrophages and almost no change in IL-6 production was noted with decreasing KCG concentration. On the other hand, IL-6 production was concentration-dependent for FUC with the 100 µg/ml FUC leading to 366 pg/ml, confirming that FUC indeed influenced macrophage polarization to M2 in contrast to KCG.

In summary, optical microscope images indicated that high concentrations of both KCG and FUC reduced cell attachment and lead to cell death. More importantly, ELISA assays showed that treatment of RAW 264.7 with FlJC resulted in a change in phenotype towards M2.

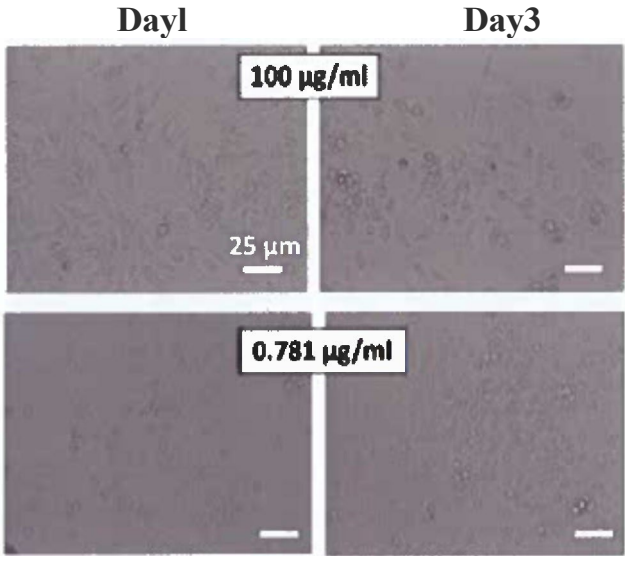


Fig. 3. Optical images of RAW 264.7 macrophages at different concentrations of FUC at days 1 and 3.

4.4. H_{202} radical scavenging assay of KCG and FUC

Elimination of free radicals is important for the efficacy of a cancer prevention agent [3◀J. The most common mechanism *via* which this occurs is through the donation of hydrogen to free radicals to convert them to non-reactive species (35]. Donation of hydrogen removes the odd electron which is responsible for radical activity. In this study, the% inhibition of free radicals by KCG and FUC was investigated using the U_2O_2 radical scavenging assay (Fig. 4E and F). For the concentration range of polysaccharides investigated, the% inhibition was found to be independent on the concentration. However, FUC displayed slightly higher 96 inhibition {approx. 75 % *vs* 70 % for KCG). Hifney et al. found that the sulphate groups in FUC are more likely to act as reductones (terminators of free radical chain reactions by donating a hydrogen atom) rather than radical scavengers to contribute to the antioxidant activity of fucoidan (36). Qi et al. proposed two possible mechanisms for the antioxidant activity of sulphated polysaccharides: one is *via* the inhibition of hydroxyl radicals formed and the second is *via* scavenging the hydroxyl radicals formed (Fig. 4G) (37).

4.5. Fabrication of PDX/KCG and PDX/FUC nano.fibrous mats and release of polysaccharides from PDX-based mats

In the current study, nanofibrous polymeric scaffolds were used for 2 main purposes: (1) as scaffold for cells to attach and proliferate promoting wound healing and (2) as drug delivery vehicle allowing the release of polysacharrides to prevent tumour recurrence. We herewith chose PDX as the major component of the scaffold as the latter has been shown to provide flexibility with comparable mechanical properties to elastin and collagen making it convenient for skin TE **(38].** In addition, the latter degrades rather rapidly under physiological conditions allowing the release of active compounds when used as drug delivery vehicle. PDXJKCG and PDX/FUC mats containing 0-30 wt% KCG or FUC were fabricated using the electrospinning method as reported previously (24J.The polysaccharides could not be loaded in higher wt% as addition of the latter to the PDX/HFIP solution drastically reduced the viscosity of the solution which negatively impacted on the electrospinnability. Indeed, blend solutions containing >30 wt% polysaccharides could not be electrospun and resulted in electrospraying. Since the preliminary objective of this study was to compare the behaviors of PDXJKCG and PDX/FUC, the range 0-30 wt% of polysaccharide was chosen. Fiber diameters of PDX/KCG and PDX/FllC mats ranged from 0.5 to 1.15 µm and 0.24-0.39 µm respectively depending on the polysaccharide content. All electrospun mats were superh.ydrophilic and the static contact angles of the mats could not be measured as the water droplet was instantly absorbed upon contact.

Skin tissue engineering scaffolds need to have comparable mechanical properties to the native skin for successful tis5Ue repair. The Young's modulus of skin differ·depending on the location. For instance, using indentation method, the Young's modulus of skin from the back and forehead **were** found to **be 83** and 35 MPa respectively [39,40). Fig. 5 shows the variation of mechanical properties of electrospun PDXJKCG and PDX/FllC mats with increasing content of the polysaccharide. The Young's modulus of both PDX/KCG and PDX/FllC decreased with increasing biopolymer content with the 90/10 composition displaying almost no change compared to pure **POX.** In fact, the Young's modulus varied in the range of 35-75 MPa. This observation indicated that the PDX/KCG and PDX/FUC blends were appropriate for skin repair in the back and forehead area. Melanomas can most often develop in areas that have had exposure to the sun, such as the back, legs, arms and face.

In contrast to Young's modulus, the maximum load, maximum stress and strain at maximum load values of the blend nanofibers were higher than that of pure PDX. These observations indicate reinforcement of the

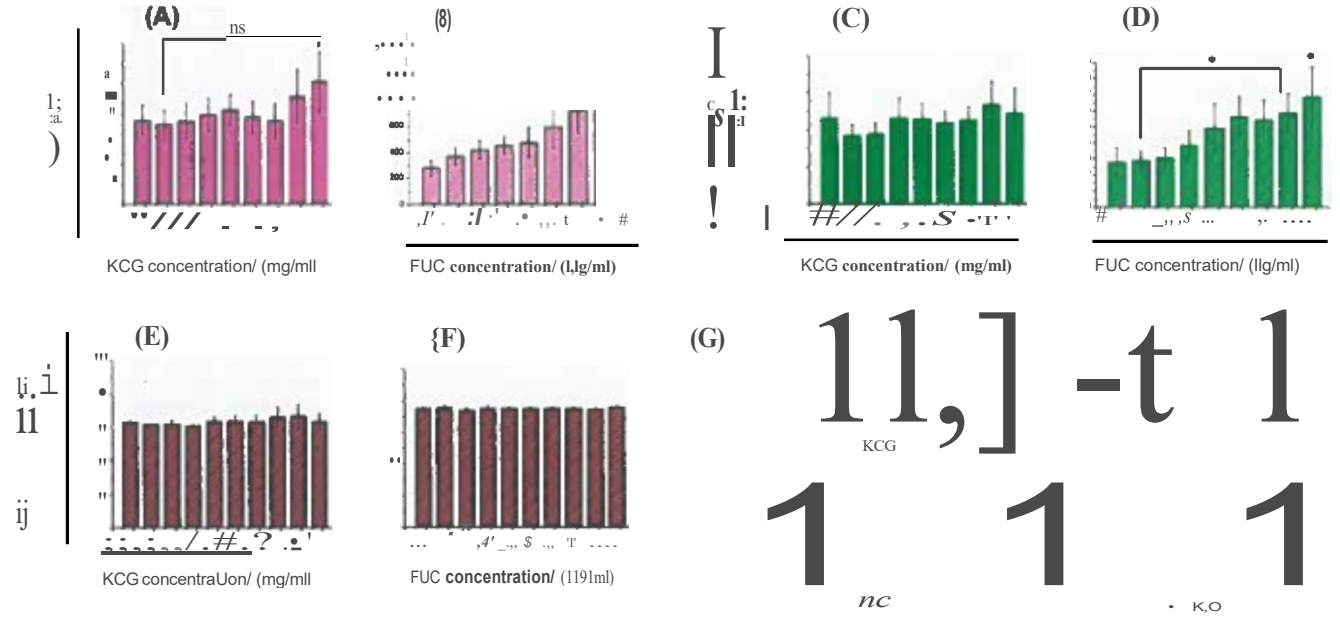


Fig. 4. Cell area {A and B) and cytoskeleton to nucleus ratio {C and D) following addition of KCG and FUC and CE and F) % inhibition of KCG and FUC following radical scavenging assay and (G) possible mechanism for radical scavenging activity of KCG and FUC. All measured values of KCG and PUC were compared with TCPS: •$p < 0.05$; "$p < 0.0001$ and (ns) not significant wherever not indicated.

Table 1
11,-6 levels measured following addition of different KCG and FUC concentrations to RAW264.7 macrophages.

Concentration of polysacchande	IL-6 concentration/ (pg/ml)
KCG	
1 mg/ml	294+17
0.Smg/ml	4.1 . 1.8
0.25mg/ml	3.9 ± 1.5
0.125 mg/ml	5.5 ± 0.9
FUC	
IOOpg/ml	366.3 ± 56.5
50 g/ml	360. 58.2
25µg/ml	177.9 + 13.0
12.5 pg/ml	111.0..20.1

nanofibrous blend matrices *via* incorporation of KCG and FUC. This may be attributed to two main reasons. First, it could be due to physical Van Der Waals interactions between PDX and the sulphated polysaccharides forming an interconnected network resisting the tensile deformation process. Secondly, the overall higher degree of crystallization of the electrospun blend fibers could be responsible for the improved mechanical properties **[24].** Indeed, Lim et al. [4 I] showed that fibrillary structured nanofibers with high degree of crystallinity provided high resistance to axial tensile forces.

4.6. Polysaccharide release kinetics

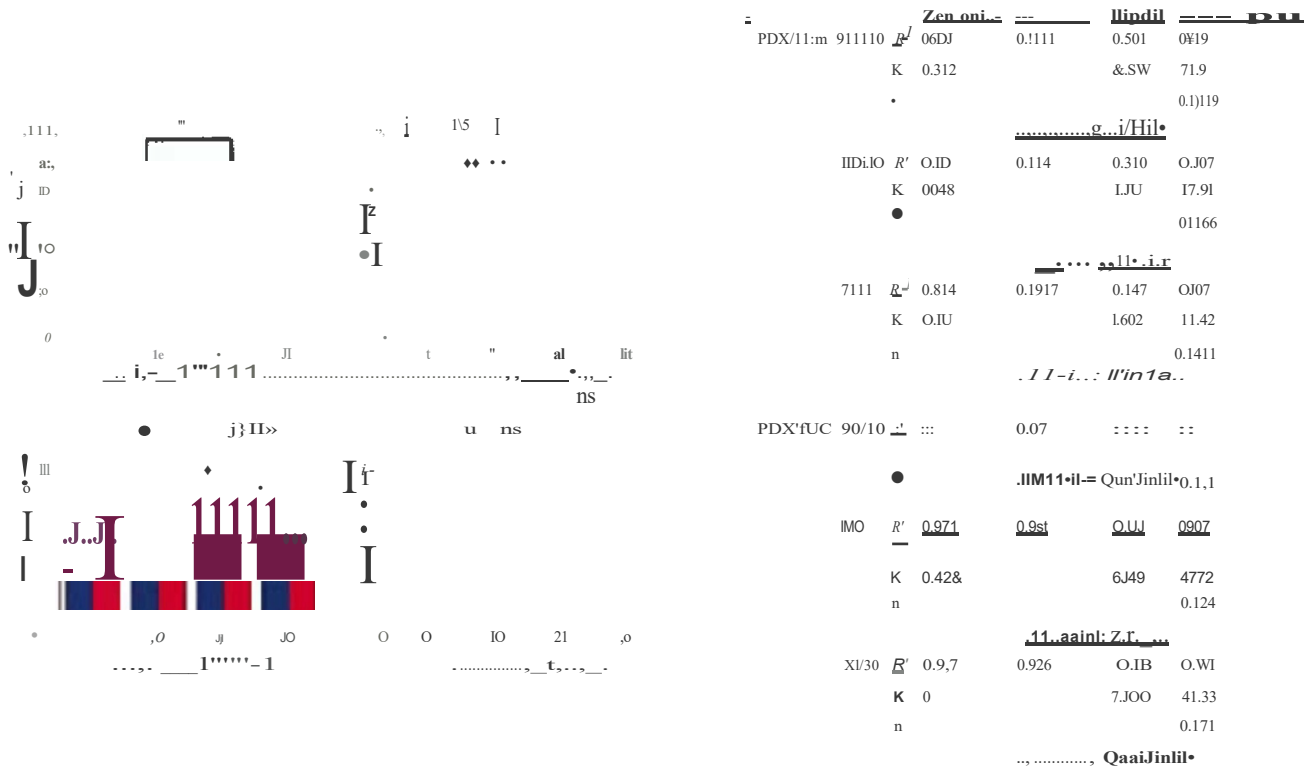
In vitro release studies of PDX/KCG and PDX/FUC mats were carried out in PBS at 37 •C over a period of 4 days. The amount of polysaccharide released (KCG or FUC) was measured *via* UV-Vis spectroscopy at different time intervals. Fig. 6 shows the release curves for different compositions of PDX/polysaccharide mats. PDX/KCG 90/10 mat released 100 % of the polysaccharide within the study period while the 80/20 and 70/30 compositions released only about 40 % of their total polysaccharide content. This may be due to the fact that the KCG was located within the PDX blend mats. On the other hand, PDX/FUC mats released almost all the FUC contained within the mats in 4 days. This observation suggests that in PDX/FUC mats, almost all FUC was located on the fiber surface. The rate of FUC release depended on the blend ratio with the 90/10 composition leading to the fastest release. For both KCG and FUC containing mats, the 80/20 and 70/30 compositions followed almost similar trends.

The release curves of KCG and FUC were fitted with zero order, first order, Higuchi and Korsmeyer-Peppas mathematical models (Table 2). According to the zero order model, release of the active agent occurs at a constant rate independent of the concentration of the active agent. ln the first order release model, release depends on the concentration of the active agent. The Korsmeyer-Peppasmodel considers non-fickian release mechanisms and is particularly applicable when more than one type of drug release phenomenon is involved. The value of the exponent, n obtained from the Korsmeyer-Peppas model can be used to derive the release mechanism whereby n $ 0.45 indicates Fickian diffusion, $0.45 < n < 0.89$ suggest non-fickian diffusion. Based on the values of n, we can conclude that most of the blend mats displayed a quasi-fickian release mechanism (Korsmeyer-Peppas model) suggesting release *via* mainly a diffusion mechanism. On the other hand, the regression coefficient for PDX/FUC 80/20 was higher when fitted with zero order equation with erosion mechanism. The release of the 80/20 mat was compared with corresponding PDX/KCG and PDXJFUC films (Fig. 6). The PDX/KCG film lost its integrity and broke down into smaller pieces after 2 h incubation in PBS compared to PDX/FUC which maintained its shape over the 96 h. Therefore, PDX/KCG film is not a good candidate for further investigation. Release of FUC from PDX/FUC film occurred rapidly and reached 100 % after only I h incubation in PBS at 37 •C.

ln addition, the in *vitro* degradation of the polysaccharide containing blend nanofibers have been assessed for a period of 5 weeks in PBS at 37 •C. *SEM* images of PDX/FUC 70/30 scaffolds following *in vitro* degradation showed some signs of fiber degradation through fiber melting in contrast to PDX/KCG where one or two areas of fiber breaking were noted **(Fig.** S3).

4.7. Inflammatory response of PDX/KCG and PDX/FUC mats

The in *vitro* inflammatory responses of the electrospun polysaccharide-containing mats was assessed by seeding murine RAW



PDX/11:m 911110	R'	06DJ	0.!111	0.501	0¥19
	K	0.312		&.SW	71.9
	•				0.1)119
IIDi.lO	R'	O.ID	0.114	0.310	O.J07
	K	0048		I.JU	I7.9l
	●				01166
7111	R'	0.814	0.1917	0.147	OJ07
	K	O.IU		l.602	11.42
	n				0.1411
PDX'fUC 90/10		:::	0.07	: : : :	: :
	●		.IIM11•il-= Qun'Jinlil•		0.1,1
IMO	R'	0.971	0.9st	O.UJ	0907
	K	0.42&		6J49	4772
	n				0.124
Xl/30	R'	0.9,7	0.926	O.IB	O.WI
	K	0		7.JOO	41.33
	n				0.171

Fig. S. (AJ Summary of mechanical properties of electrospun PDX/KCG and PDX/FI.IC mats. All measured values of PDX/KCG and PDX/FUC were compared with PDX: •$p < 0.05$; .. $p < 0.0001$ and (ns) not significant wherever not indicated and (B) Results of mathematical modeling for KCG and PUC release kinetics from blend mats.

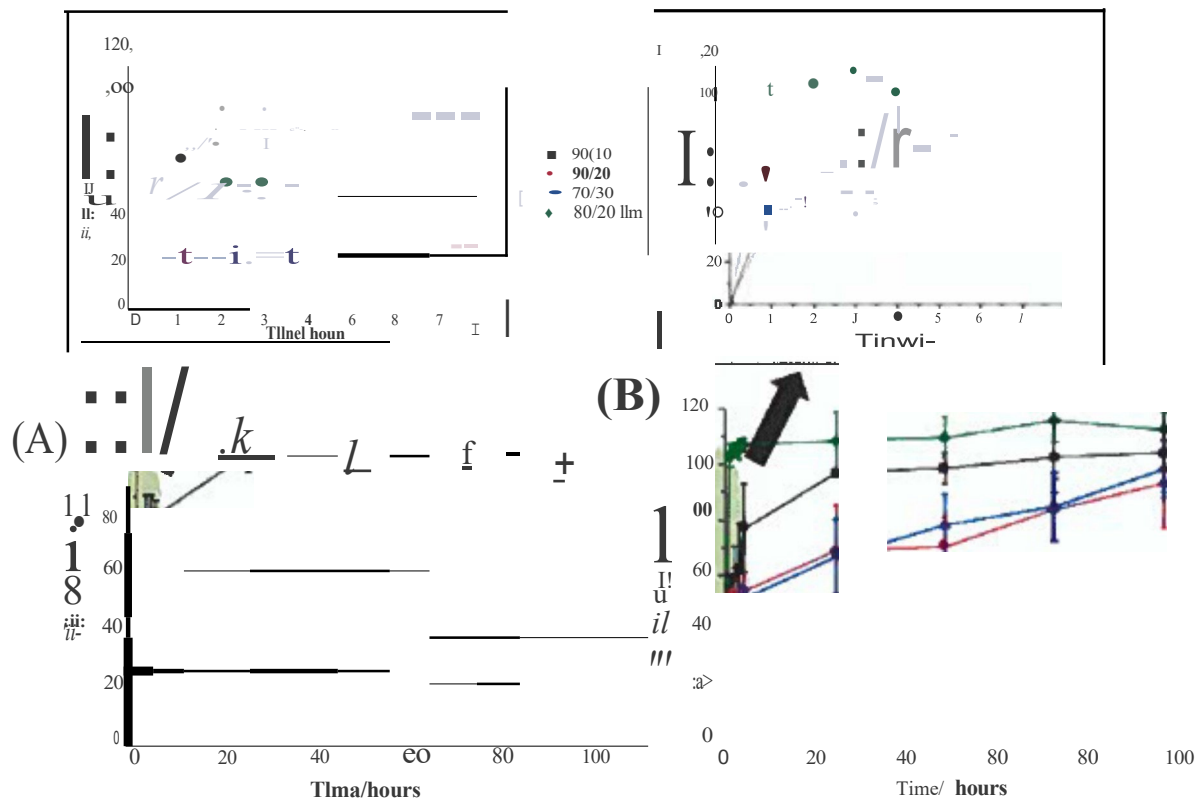


Fig. 6. /11 vitro polysaccharide release from PDX/KCG and PDX/FUC mats in PBS at 37 •C.

Table 2
Identity or scaffolds for ill *vivo* wound healing studies

Sc•ffold label	Identity
	Negative conlrol
JI	**Positive control**
III	POX
IV	PDXII<CG 70/30
V	PDX/F\JC 50/50
VJ	PDX/FUC 50/50 + CUR
VII	PDX/F\JC 70/30 + CUR
VIII	PDX/F\JC 70/30 + CUR + MH

264.7 macrophage cells. **SEM** images showed that the cells adopted a nanened shape with no ruffles with increasing KCG and FUC contents (Fig. 7A-B). Ruffles present on the cell surface Indicated the process of macroplnosorne fonnation. Indeed, close analysis of the SEM images shows the presence of rnacropinosomes (for fluid intake) with average diameter of 0.61 11m on several cells at low KCG and FUC contents (0 and 10 wt%). At higher polysaccharide content, no macropinosome was noted probably due to cytotoxic property of the former. The first step Involves the formation of actin veils **through** erected tent pole structures **[42].** The tent poles then meet resulting in drcularization of the ruffles. Finally, the veil collapses in synchrony with crossing over and twisting of tent poles leads to macropinosome formation. AJI 3 steps could be observed on the surface of cells cultured on PDX/KCG and PDX/FUC (100/0 and 90/10). All scaffolds showed signs of macrophage mediated degradation as noted by fiber thinning and uneven fiber surfaces.

From SEM images, the extent of F-actin rich membrane protrusions were calculated by determining the average ruffling scores (minimum 0 and maximum 3) of at least 20 cells. It could be noted that the ruffling index decreased with increasing polysaccharlde content possibly due to cytotoxicity caused by the latter (lg. 7H).

In order to better visualize the cytoskeleton of macrophages, the latter were stained for their nuclei and f-actin filaments using DAPI and fluorescently labelled phalloldin, respectively. An increase in macrophage cell area and actin edge intensity show a change to the anti-inflammatory and pro-healing M2 phenotype [31]. The cell area and actln edge intensity was quantified using CellProfiler when cultured on different scaffolds showed an Increasing trend with increasing polysaccharlde content irrespective of whether It was KCG or FUC **(Fig.** 71 and J).

In addition, the amount of the pro-inflammatory cytokine TNF•o: released in cell culture supematants was quantified using ELISA (**Fig.** 7K). In general, addition of KCG to PDX resulted in a decrease in the amount of TNF-<1 while incorporation of FUC led to an increase in the amount of TNF-<1.

4.8. In vitro studies on PDX/KCG and PDX!FUC nano.fibrous :scaffolds

In vitro cell culture studies were carried out using human uveal melanoma MP 41 and murine fibroblasts L 929 under two different conditions {1} using the electrospun mats as drug delivery vehicles and (2) using the electrospun mats as for tissue regeneration and as drug delivery vehicles. The rationale for this ls that the electrospun blend scaffolds are intended for topical and local application following skin tumour removal at the site of the wound.

- On electrospun mats acting as both drug releasing systems and cell supports

To assess this particular aspect, either MP 41 or L 929 cells were seeded on the electrospun mats and the % cell survival was quantified after 7 days using the live and dead staining method (fig. 8A and B). To have more in,depth detail on cell morphology, both **MP** 41 and L 929 cells on the scaffolds were fixed as detailed in the experimental section and viewed under the scanning electron microscope (SBM).

Llve and dead staining results showed that all the electrospun mats inhibited MP 41 proliferation(%cell survival <11 % for all blend mats) in contrast to pure PDX. MP 41 cell number after 7 days was much lower than the initial cell seeded number **(i.** 20,000) implying KCG and FUC released from the mats were toxic to the cells. The% cell survival did not show a direct correlation with KCG or FUC blopolymer content indicating that cell death was dependent on the amount of polysaccharide being released by the blend fibers.

On the other hand, L 929 proliferated well on all PDX blend mats and the% cell survival of L 929 was slightly higher on electrospun PDX/KCG mats compared to pure PDX and PDX/FUC while the % cell survival for PDX/FUC ranged between 60 and 100 % depending on the blend ratio and amount of FUC.

SBM images revealed that the MP 41 cells adopted rounded shapes on all PDX/biopolymer blend mats In contrast to TCPS where they were elongated in shape. Multicellular spheroids with grape-like morphologies could be noted on ali the electrospun blend mats **(fig. 8E).** This indicated that the blend scaffold surfaces do not favour cell material interactions and instead promoted cell-cell cross-talks as may be noted from the SEM images (**Fig.** 7E}.The size of these 'multicellular grape-like

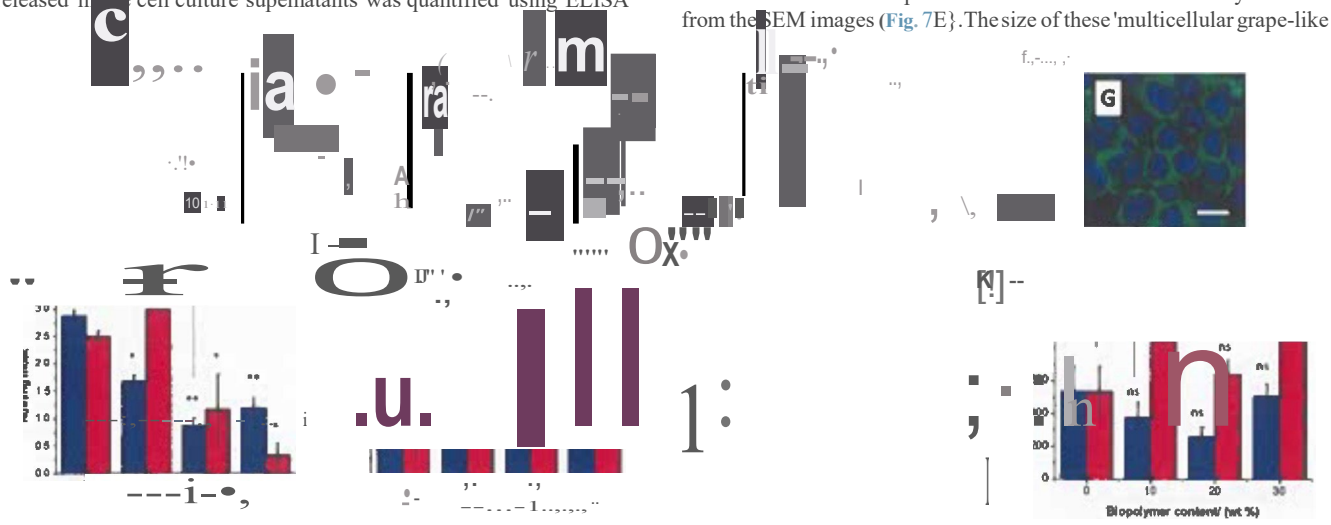


Fig. 7. SEM images of RAW264.7 cells cultured on (A) PDX, (B) PDX/KCG 90/10, (C) PDX/KCG 70/30, (D) PDX/FUC 90/10, (E) PDX/FUC 70/30 (F) fibers showing macrophage mediated degradation, (G) Fluorescence microscopy image showmg nucleus in blue and cytoskeleron ln green, (H) Summary of ruffling indices, (I) Summary of cell area on different scaffolds, (J) Summary of actin edge intensity and (K) concentration of TNF- 11 produced by cells after 24 h. All measured values corresponding to PDX/KCG and PDX/FUC were compared with PDX: •$p < 0.05$; .. p 0.0001 and {ns) not significant wherever not indicated.

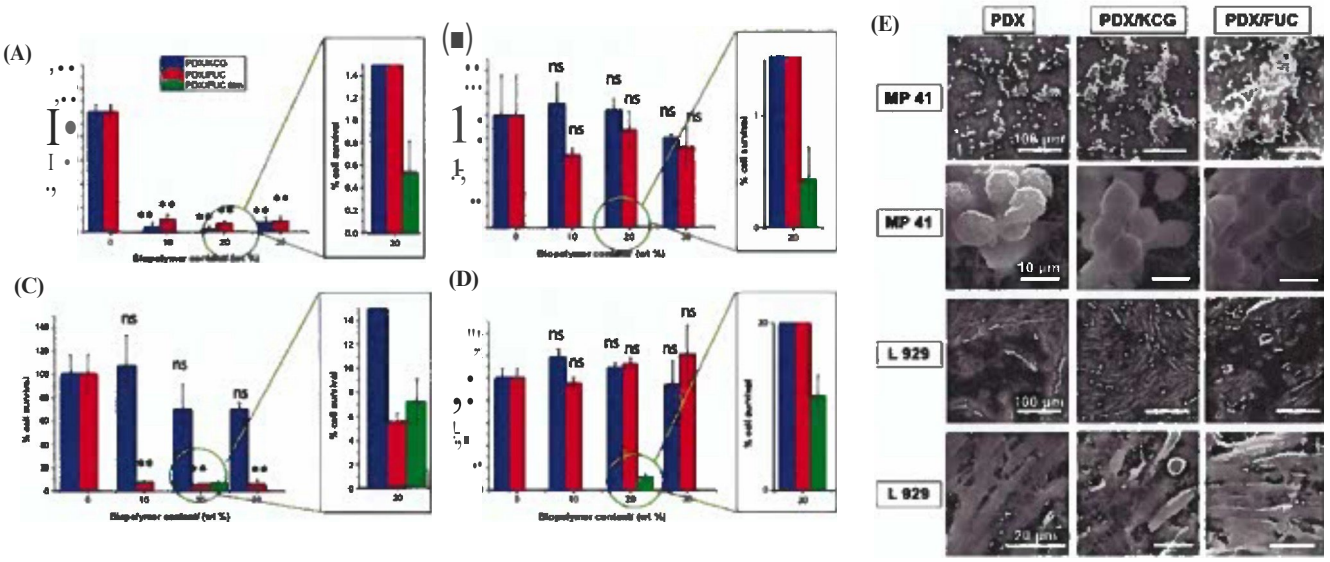


Fig. 8. % survival of (A) MP ◄1 cells and (B) L 929 cells seeded on PDX/KCG and PDX/FUC scaffolds following *7* days,% survival of (C) MP 41 cells and (D) L 929 cells not in direct contact with PDX/KCG and PDX/FUC scaffolds following *7* days (E) SEM images showing morphology of MP 41 and L 929 cells on electrospun mats after *7* days. All-measured values were compared with TCPS: •$p < 0.05$; ...$p < 0.0001$ and (ns) not significant wherever not indicated.

spheroids' were larger on POX/KCG {average area 4001 ± 1229 μm^2) and POX/FUC{average area 40,333 ± 10,242 μm^2) compared to those on POX {average area 1791 ± 1013 μm^2) implying that the electrospun blend mats favoured the clustering of **MP** 41 cells. In addition, membrane ruffling was observed on the dorsal surfaces of cells cultured on POX in contrast to POX/KCG and POX/FUC. Cell membrane ruffling is a dynamic and rapid movement consisting of the extension and withdrawal of cell membrane protrusions. Membrane ruffling has been shown to relate to the invasive and metastatic potential of tumour cells by promoting cell migration through the formation of new focal adhesions [43]. This suggested that the invasive potential of MP 41 cells is reduced when cultured on electrospun blend PDX/KCG and PDX/FUC mats, in line with previous results which showed that both KCG and FUC reduced the migration of MP 41 cells {Flg. 2). L 929 cells, on the other hand, adopted similar morphologies on POX as well as on blend mats and on TCPS *Le.* elongated morphologies with well spread shapes (Fig. 8E}. The cells showed a tendency to align in one direction. Magnified images shown interaction of the L 929 cells with the nanofibers for all blend mats and POX.

Overall, live/dead staining results indicated that even if residual cancer cells could be present in the wound area in contact with the scaffold, they would not multiply and proliferate. Instead, the biopolymers released from the electrospun mats lead to cancer cell death. Morphological analysis *via* SEM showed reduced metastatic potential of MP 41 cells on blend mats. The insignificant cytotoxlcity of the blend mats to L 929 fibroblast cells suggest that the electrospun mats would not impede wound closure.

- Using electrospun mats as floating drug eluting cell supports

The influence of the biopolymer-releasing blend fibers on cells far away from the scaffold was investigated by using the set-up depicted in Scheme I whereby 2 stainless steel rings were used to hold the mats on top on the cell monolayer ensuring that the cells were not in direct contact with the scaffold. Briefly, the cells were seeded directly in TCPS well plates and after allowing 3-4 h for cell attachment, a first stainless steel ring was placed over the cell monolayer followed by the scaffold which was sandwiched between another stainless steel ring. Results summarized in Fig. SC showed that POX/FUC scaffolds were more cytotoxic to MP 41 cells compared to similar weight ratio PDX/KCG mats. This was in line with previous results which confirmed the higher toxicity of FUC to MP 41 cells in contrast to KCG (**fig.** I).

We also assessed the effect of KCG and FUC released from the blend mats on murine fibroblasts L 929 cells not in direct contact with the scaffold (Fig. 80). From Fig. 8D, it could be observed that POX/KCG was not cytotoxic to L 929 cells although POX/FUC promoted cell proliferation more than POX/KCG. This interesting observation supported the use of POX/FUC over POX/KCG mats as drug delivery vehicle targeting residual cancer cells and also as cell support for healthy cells promoting wound healing.

4.9. In vivo immune response studies using albino Wistar rats

4.9.1. In vivo biocompalibility

To investigate the foreign body response elicited by the electrospun blend mats, the latter were implanted in the dorsal region of adult albino Wlstar rats for a period of 2 weeks. Electrospun POX scaffolds was used as the control. All scaffolds were first disinfected using 70 % ethanol followed by three PBS washes before being implanted into the dorsal subcutaneous pockets. Three layers of electrospun mats were placed in each pocket and the pocket was then closed using an intradermal PLGA 4/0 suture. The rats were followed over the whole period of study for any signs of inflammation such as redness, swelling, *etc.* at the implantation site. The weight of the rats were also noted over regular time intervals to ensure their healthy status. None of the rats displayed any behavioural change or visible signs of Inflammation and physical impairment. After 2 weeks, the scaffolds were removed layer by layer in some of the rats for SEM imaging and labelled as exterior layer (E), middle layer (M) and interior layer (0 while In the remaining rats, tissue sections with the scaffolds were retrieved for histology analysis. Cells of various morphologies could be noted on the surfaces of the exterior and interior layers of all scaffolds (fig. 9A}. For the POX mat, a thick tissue layer covered the surface of the interior layer. Comparing the middle layer of POX, POX/KCG 80/20 and POX/FUC 80/20 scaffolds, it can be noted that PDX/KCG 80/20 mat led to the highest number of infiltrated cells compared POX/FUC 80/20 where abnost no cells could penetrate. This can be rationalized by the fiber diameter of the electrospun mats. Indeed, fiber diameters of POX and POX/KCG mats were much larger than PDX/FUC (1 μm vs 0.21 μm) suggesting larger pore sizes in PDX and PDX/KCG which allowed cells to infiltrate within the mats.

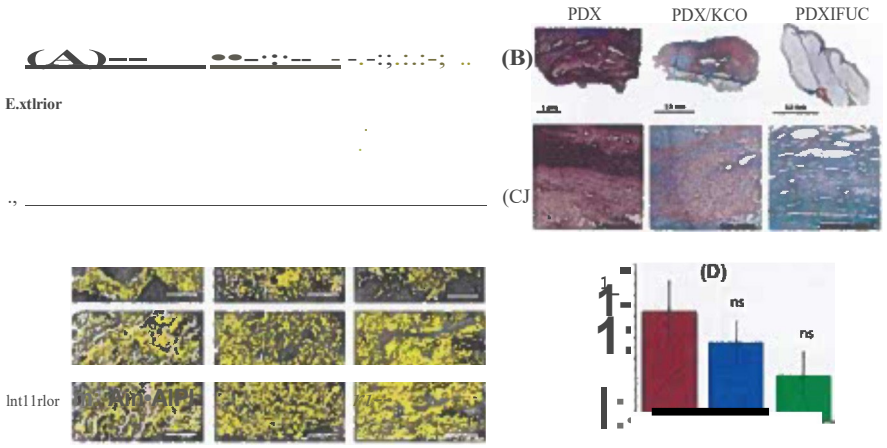


Fig. 9, (A) SEM images of retrieved scaffolds after 2 weeks ill *vivo* implantation, **(B)** Masson·s trichrome images of tissue sections, (C) Magnified Masson's trichrome images depicting the composition of fibrous capsule and (D) quantitative analysis of fibrous capsule thickness. Fibrous capsule thickness of PDX/KCG and PDX/FUC were compared with PDX: •p < 0.05; ••p < 0.0001 and (ns) not significant wherever not indicated.

Fibrous capsule formation was noted around all electrospun scaffolds (Fig. 9B). There were significantly more cells in the fibrous capsule surrounding PDX/KCG 80/20 compared to those around POX and POX/FUC 80/20 which consisted mostly of collagen fibers (Fig. 9C). Quantitative analysis of Masson's trichrome images showed that the addition of polysaccharides KCG and FUC reduced fibrosis around the scaffolds suggesting improved host-scaffold integration (Fig. 9D). Compared to KCG, the incorporation of FUC led to thinner fibrous capsule formation suggesting that the latter causes reduced immune response in the rats.

Masson·s trichrome images of removed tissue and scaffold samples after 2 weeks indicate varying extent of degradation (Fig. 9B). In particular, the POX and PDX/KCG 80/20 scaffold showed major signs of degradation with thinning of the scaffold layers due to larger pore diameters compared to PDX/FUC 80/20. The three scaffold layers could no longer be differentiated as they broke down Into several smaller pieces. On the other hand, all 3 layers of PDX/FUC 80/20 mats could be easily identified and showed almost no sign of degradation. Overall, we conclude on the faster *in vivo* degradation of PDX and PDX/KCG 80/20 in contrast to PDX/FUC 80/20 as a result of larger fiber diameters and therefore larger pore sizes allowing for physiological fluid penetration.

4.9.2. In vivo wound healing

Following *in vitro* and *in vivo* biocompatibilitystudies, 10 electrospun scaffold mats were chosen for further *invivo* wound healing studies using Wistar rats as models. *In vitro* studies showed that PDX/FUC had better wound healing potential than PDX/KCG, supporting the cytocompatible properties of FUC. The latter did not impede fibroblast migration and promoted macrophage polarization to M2 phenotype. Based on these results, a blend containing higher amount of FUC was fabricated *i.e.* PDX/FUC 50/50 to maximize the benefits of FUC. Some of the chosen scaffolds were also loaded with small natural molecules such as curcumin{CUR), and manuka honey **(MK)** (T;1ble 3). Curcumin possesses anti-inflammatory and anti-oxidant properties and studies have shown that it

Table 3
Identity of scaffolds for ill *vivo* wound healing studies.

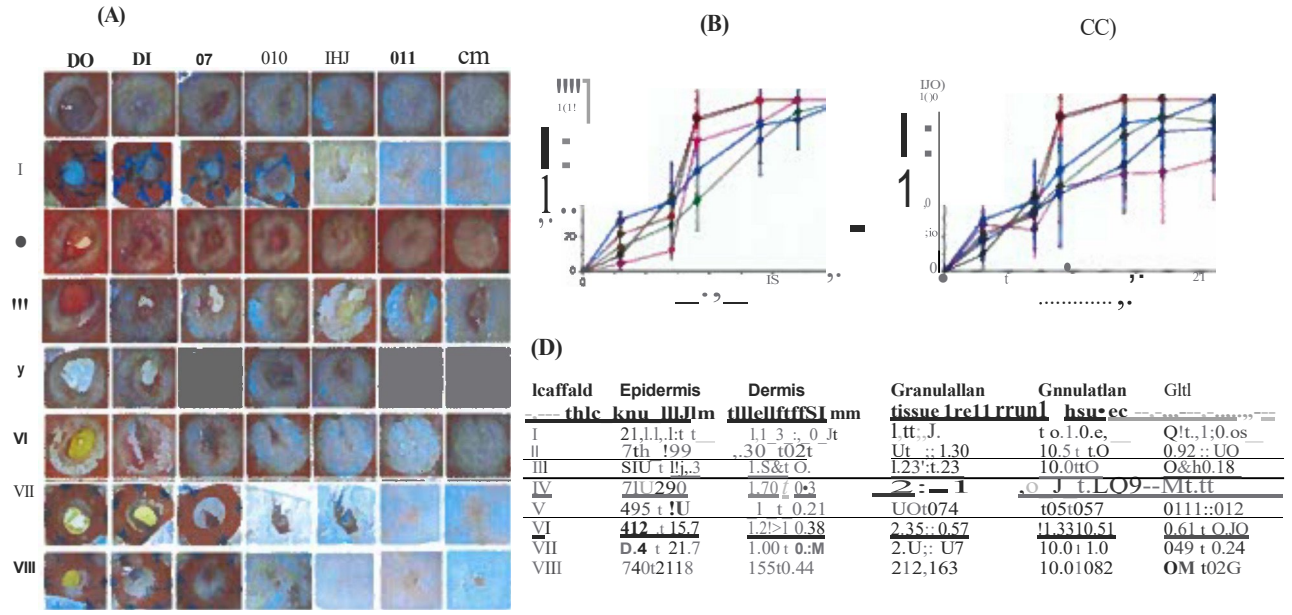
Scaffold label	lden1ity
	Negative ronttol
II	Posllive control
Ill	PDX
IV	POX/KCG 70/30
V	PDX/FUC 50/50
VI	PDX/FUC 50/50 + CUR
VII	PDJUFUC 70/30 + CUR
VIII	PDJUFUC 70/30 + CUR MH

enhances granulation tissue formation as well as collagen deposition during the remodeling process **[44).** Several studies have concluded on the benefits of manuka honey in wound heahng. Its hydrogen peroxide content helps to eliminate bacteria in the wounds and stimulates vascular endothelial growth factor {VEGF) production. In addition, its low pH {3.5--4) decreases protease activity, increases oxygen release from haemoglobin, and stimulates macrophages and fibroblasts in the inflammatory and proliferative phases respectively [45).

The commercial scaffold Seeskin (collagen sheet) and gauze was used as positive and negative controls respectively. The protocol for carrying out the wound healing studies was similar as reported previously whereby 6 mm diameter wounds were created on the dorsal region of rats [29]. Silicon donut shaped wound splints were sutured around the wounds to prevent dosing of the wounds *via* contraction. All electrospun mats were first hydrated in normal saline before being placed on the wounds. From Fig. l0A, we note that both the positive and negative control wounds closed completely after 21 days. However, the negative control started contracting significantly as from day 7 losing its circular shape and adopting an elongated shape. Similarly, the positive control also displayed contraction and became star-shaped at day 10. All remaining scaffolds groups healed completely except for scaffolds VI and VII and led to scarless wound healing apart from scaffold VI. The graphs of% wound closure *vs* time {**Fig.** 1OB) show that both the positive and negative control follow a similar trend with rapid wound closure whereby 70 % of the wound was closed within 9 days. In contrast, most of the electrospun mats healed at a slower rate whereby <40 % of the wound was healed by day 9.

Tissues were harvested from the healed wound sites for the various scaffold groups and stained with Masson's trichrome and picrosirius red stains. Granulation tissue scoring and global healing indices (Gl-ll) were determined from the histological Images [29]. Among all scaffolds, mat V displayed the highest global healing index and smallest granulation tissue area indicative of good overall healing. Comparing the data corresponding to scaffolds IV and V in Fig.1 OD we can conclude that FUC improves the wound healing compared to KCG as noted by the lower GT area and higher GHI. Incorporation of both CUR and MH within the scaffolds reduced the granulation tissue area and improved the GHI.

The last stage of wound healing involves the ECM remodeling process whereby the formation of granulation tissue stops and the ECM components undergo several changes. For instance, collagen III is replaced by collagen I. The angiogenic processes are also reduced with a slowing of the overall metabolic activity at the wound site **[4b].** Masson's trichrome images showed that the distance between collagen fi. brils in the granulation tissue varied depending on the scaffold used. In



lcaffald	Epidermis	Dermis	Granulallan	Gnnulatlan	Gltl
thlc knu lllJJm	tllleliftfffSI mm	tissue 1re11 rrun1	hsu• ec		
I	21,l.l,.l:t t	l.1_3 :, 0_Jt	l.tt;,J.	t o.1.0.e,	Q!t.,1;0.os
II	7th !99	,.30 t02t	Ut :: 1.30	10.5 t tO	0.92 :: UO
III	SIU t l!j,.3	1.S&t O.	1.23':t.23	10.0ttO	O&h0.18
IV	71U290	1.70 f 0•3	2:_1	,o J t.LO9--Mt.tt	
V	495 t !U	1_t 0.21	UOt074	t05t057	0111::012
VI	412 t 15.7	1.2!>1 0.38	2.35:: 0.57	!1.3310.51	0.61 t O.JO
VII	D.4 t 21.7	1.00 t 0.:M	2.U;: U7	10.0 t 1.0	049 t 0.24
VIII	740t2118	155t0.44	212,163	10.01082	OM t02G

Fig. 10. **(A)** Images of wounds over 21 days, **(B)** and {C) % wound closure with time, {D) summary of histological analysis.

particular, the negative control and the PDX group resulted in comparable values while the positive control and the scaffold group had almost similar values **(Fig.** S2).

4.10. *Preliminary* in *vivo anticanur effect as nanoscaffold patch*

Athymic female nude mice models were used to test the efficacy of the prepared nanofibrous scaffolds in vivo. Subcutaneous tumours were induced and allowed to develop for 4 weeks in nude mice. The tumour sites were then covered with the nanofibrous mats PDX and PDX/FUC or left untreated. After 4 days treatment, the mice were sacrificed and the tumour volume were measured. It is important to note that since the FUC concentration in the nanofibrous mat is high and the release kinetics from the in *vilTo* study showed a rapid release pattern with an initial burst, we hypothesized that 96 h treatment would show some treatment efficacy on the solid tumour.

Interestingly, treatment with PDX/FUC nanofibrous mat displayed tumour reduction of 7.14 % within 96 h of treatment compared to the control with 11.31 % increase in tumour volume within the same time interval. Moreover, treatment with POX mat exhibited twnour regression of - 2 % lesser tumour growth compared to the negative control (untreated mouse).

H&E staining was performed on the excised tumour tissues and on the main organs (liver, spleen, lung) to investigate the antitumor efficacy of nanofibers and its possible toxicity (**Fig.** 11). In the tumour sections, 45 % 30 % and 50 % central coagulative/liquefactive necrosis were noted in the PDX, PDX/FUC nanofibrous mat treated and untreated mice respectively. Small groups of necrotic calcified cells were found in the PDX/FUC treated mice, evidencing the effectiveness of FUC-release and the antitumor activity of FUC from the nanofiber scaffolds. **Areas** of moderately increased stromal fibroblastic tissue were visible adjacent to the necrosis in both mice treated with PDX and the one left untreated (control) in contrast to the PDX/FUC treated one which showed only mlld focal fibroplasia.

consisting of increased spindle cells in the stromal tissues adjacent to the necrosis. No decrease in the number of actively dividing cells were noted in the tumour tissues of the PDX/FUC treated mice. No signs of peripheral lymphocytic inflammation was noted in the PDX/FUC treated mouse compared to mild-moderate Inflammation in the negative control mice.

Assessment of the liver showed that the PDX/FUC treated mouse had normal hepatocytes while the negative controls displayed mild cytoplasmic vacuolisation of centrilobular hepatocytes and the presence of fibrin material or fibrillar serum-like material within the lumens oflarge blood vessels.

Therefore, it isarguably compelling that the FUC-loaded nanofibrous mat showed some anti-cancer potential and can be optimised for robust anti-tumour efficacy if tested for a longer period. Also, it will be interesting to assess and ascertain its wound healing activity along its anticancer activity as a superlative modality for cancer treatment and tumour regeneration prevention. It has been reported that M2 polarized macrophages can cause immunosuppression through the secretion of anti-inflammatory factors, through angiogenic and lymphangiogenic regulation, hypoxia induction which can promote tumour proliferation and metastasis (47]. However, despite being anti-inflammatory, such outcomes were not observed with FUC loaded scaffolds.

5. Conclusions

In the current study, KCG and FUC loaded nanofibers were fabricated for the sustained release of the polysaccharides KCG and FUC in the tumour vicinity. Most of the blend mats displayed a quasi-fickian release mechanism which fitted to the Korsmeyer-Peppas model, suggesting release mainly *via* a diffusion mechanism. Addition of KCG and FUC to POX reinforced the nanofibrous matrices due to physical Van Der Waals interactions between PDX and the sulphated polysaccharides and due to improved crystallization in the blend fibers. *In vilTo* studies showed the formation of multicellular spheroids with grape-like morphologies following seeding of **MP41** cancer cells on all the electrospun blend mats, Indicating that the blend scaffold surfaces promoted cell-cell crosstalk instead of cell-material interactions. Lower degree of MP41 cell membrane ruffling suggested reduced invasive potential of the cells when cultured on electrospun blend PDX/KCG and PDX/FUC mats in line with previous results which showed that both KCG and FUC reduced the migration of **MP 41** cells. Toxicity of KCG and FUC released from the mats could be confirmed from the lower number of **MP41** cells on the blend mats 7 days after initial seeding. M'IT assay and SEM images confirmed that the blend mats were non-cytotoxic to L929 fibroblasts. Overall, these results indicate that upon application to the tumour resection site, the PDX/KCG and PDX/FUC mats will be able to kill any

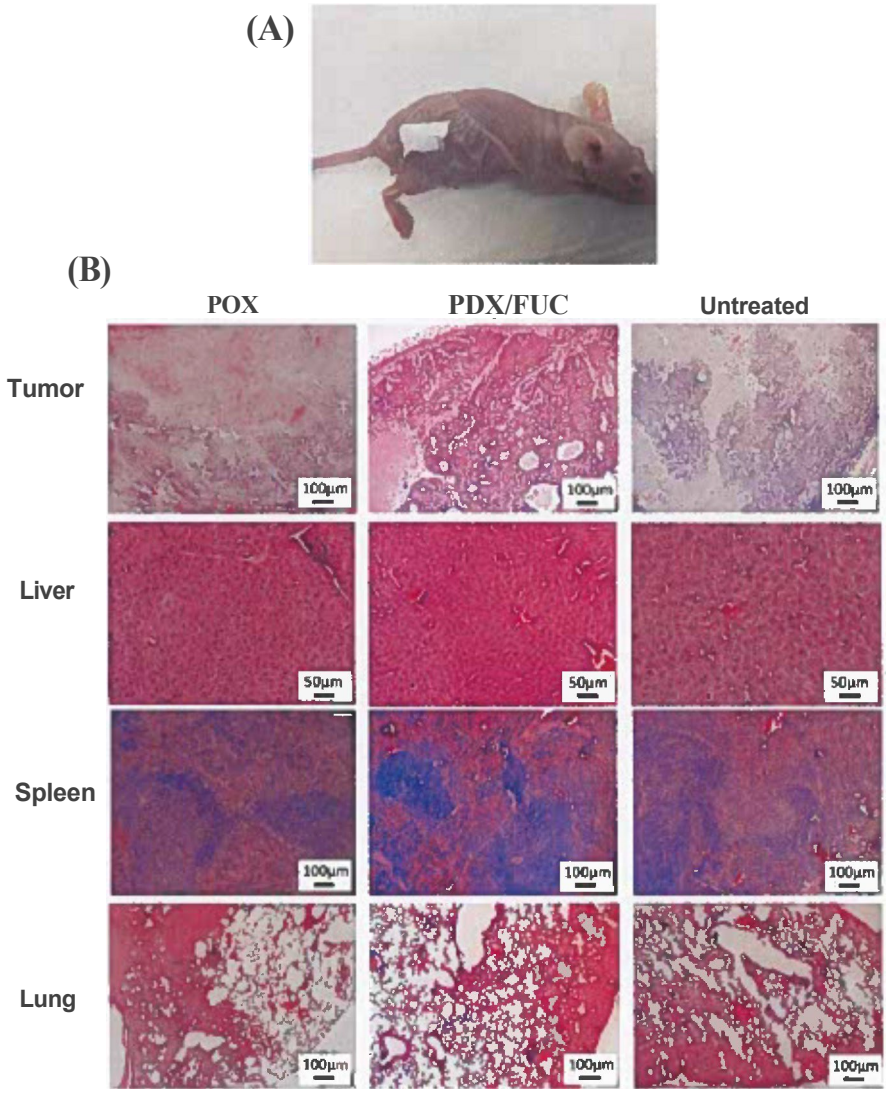


Fig. 11. (A}Photo showing application of nanofibrous patch over tumour and (B) Histology images showing tumour, liver, spleen and lung tissue sections following either treatment with nanofibrous patch or when left untreated.

residual cancer cells while simultaneously not impairing wound closure, but rather accelerating the healing process. Following *in vivo* implantation in rats, none of the scaffolds caused significant inflammatory reaction and all of them led to fibrous capsule formation with PDX/FUC forming the thinnest capsule. Wound healing studies showed that FUC improved the wound healing more compared to KCG as noted by the lower GT area and higher GHI. Results from the conducted in vivo prestudy indicated anti-cancer potential of the fabricated PUC-loaded nanofibrous mat. However, this interesting observation still needs to be further validated. Further in *vivo* study is required to assess the dual anticancer and wound healing potential of the nanofibrous patches. The fabricated nanoflbrous patches are an addl tion to our innovative work in cancer nanomedkine, and aims at circumventing the limitations of conventional chemotherapy in melanoma management.

Funding

ABL thanks RT Knits Ltd. (Mauritius) for funding RCA project vote KB027. YEC thanks the National Research Foundation (NRF) of South Africa for the SARChl Grant.

CRediT authorship contribution **statement**

Nowsheen Goonoo: Writing - review & editing, Writing - original draft, Visualization, Methodology, Investigation, Formal analysis. **Fanny** Gimie: Investigation. **Imade Ait-Arsa:** Investigation. **Melanie Ziman:** Writing - review & editing, Resources. **Samson A, Adeyemi:** Methodology, Investigation. **Philemon Ubanako:** Investigation. **Lindokuhle M, Ngema:** Investigation. **Yahya** E, **Choonara:** Writing review & editing, Supervision, Resources, Project administration. **Archana Bhaw-Luximon:** Writing review & editing, Writing original draft, Resources, Project administration, Methodology, Funding acqulsltion, Conceptualization.

Declaration of competing interest

The authors declare the following financial interests/personal relationships which may be considered as potential competing interests: Archana Bhaw-Luximon reports financial support was provided by RT Knits Ltd. Yahya &sop Choonara reports financial support was provided by National Research Foundation South Africa.

Data availability

Supplementary file attached.

Acknowledgements

NG would like to thank RT Knits ltd for her postdoctoral fellowship.

Appendix A. Supplementary data

Supplementary data to this article can be found online at https: /doi org/10.1016/j.bioadv.2024 213870.

References

(I I Z. Yuan, K. Zhang X. Jiao Y Cheng, Y Zhang, P Zhang, X Zhang, Y. Wen, A cnntrollable local drug delivery synem rn>sed on porous fibers for syncrg1SUc treatment of melanoma and promoling wound healing, Biomaler. Sci. *1* (2019) 5084-5096

(2) P.A. van der !:erd,n, P.J.M Lohuis, A.A.II.I Hart, W.C. Mulder, H Vuyk, Secondary in1en1ion heal,ng after excision of nonmelanorna skin cancer or 1he head and neck: Slatislical evaluation of prognostic values of wound characlemhcs and final cosmetic resull5, Plasl. Reconstr Surg. 122 (2008) 1747-175.'\.

(3) D. Simoes, S.P. Miguel, M.P. Ribeiro, P. Cou1inho, A.G. Mendon •. I J Cortfoa, **Recml Hdvances on an1imicrobi;:1I wound dressing: review. Eur. J. Ph.lrm** Riopharm. 127 (2018) 130-141.

141 A. Manka, A.M Di, Silva, **A.M.** Cardoso, **M.** Moreno O.B Leal, A. Dutra 0. Silva. M.R.C Schcun er, V **M.M** Monch, M.D Bagaunl. lligh levels or exiracellular ATP lead lo chronic innammatory response in melanoma patienl5, J Cell Bicx:hem 119 (2018) 3980-3988.

(51 I..K. Jacobson, M.B. Johnson, R.D. D.wh1a, S. N1kMm-8'enia, A I(. Wong, Impaired wound healing after radiation lherapy. • systematic review of pathogenesis and lrealmenl, JPRAS Open 13 (2017) 92-105.

[6) N. Goonoo, A. lloodhun, M. Ziman, E. Gray, A Bhaw-Luximon, Repw-posing nano t11ablfd polymeric scAffolds for 1un1or-wound managemenl and JD lwnor **enginmring**. R gen. Med 15 (2020) 2229-2247,

(7) **R. B.** Rlgon, **M.** H. Oyafuso, **A.** T. Fujimura, M. L. Go ez, A.H. **do l'nldo**, M. P. D. Gremiio and M. ChorlDi, Nanottcltnology-based dn13 delivery Systems for Melanoma AnlitWDDTAI Thmipy: • review. Biomed. Res. Int., 2015, 2015, 841817.

(8) S Vishnubhakthula, R Elupul.l, P..F. Dur n-Lara, Reccnl advances in hydrogel• based drug delivery for melanoma Cancer lherapy • Mino review, J Drug IJehv 2017 (2017) 7275985.

(9) JE. Pal11tr1 . V. Arcadio, S. D Arnone, M. Biasiucci G. Gigli, 8. Cortese, Therapeutic l'CL scaffol<l for reparation *of* resected osteosarcoma defeel, Sci. Rep. 7 (2017) 12672.

(101 Q. Yu Y. Han, T. Tian, Q. Zhou, Z. Yi, J. Chang, C. Wu, Chinese sesame stick• inspired nano-fibrous scaffolds *(or* tumor 1herapy and skin tissue reconstruc1lon, 81omalerials 194 (2019) 2.S-35.

1111 N Oliy•ei, M. Moosavi-Nasab S.M Mazloomi, Therapeutic act1v11)' of fucotdan and carrageenan as marine algal polysaccharides against viruses. *3,* Biotech 12 (2022) 154.

ll2J **M.** Khotimchenl<o, V. Tiasto, A. Kahlnik, M Begun, R. Khotimchenko, E. Leon,..va. 1 Bryukhovel5kiy, Y. Khotimctienko, Antilumor potential of cartagetMns **frOfll** marine red algae, Carbohydr. Polym. 146 (2020) 116568.

(13) **Z.**Liu, T. Gao, Y. Yang, F. Meng, F. Zl\an, Q. Jlang and X. SUn, Anti-cancer ActJvity of **Porphyran and Carrageenan** from **Red Seaweeds. Mol«ules,** 001:10. 3390. molecules2◀234286.

[14) A. Kasai S. An(uka, N. Koshiba, D. Takahashi, K. Toshima, Syslent"lk synthesis of (o,.-molecular weight fucoid•n derivaiives and their effe<t on cancer ceUs Of!. Biomol. Chem 13 (2015) 10556-10568.

(15) H. Yuan, J. Song, X. Li, N Li, S. Liu, Enhanced immunoslimulalory and •ntitumor ac1ivi1y of d1fferen1 derivailves of ,-carrageenan ollgosaccharides from Kappaphycus <triatum, J Appl. Phycol 23 (2011) 59-65.

(16) E.S. Pra,edya, M. Miyake, IJ. Kobayashi, /\. Hazama, Carrageenan delays cell cycle progression in human cancer cells In vi1ro demonstraled by FUCCI 1mag1ng, BMC Complement. Ahem. Med. 16 (2016) 270.

[17) N Ung, Growth inhibition and cell cycle arrest of kappa•Selenocarragoenan **and** pachtaxd on llepG2. cells, AMR 343-344 (2011) f>J0-534

118) T.•J. Pan, L-X. Li, J.-W. 2hang, Z.-S Yang, 0.-M. Shi Y.-1<. Yang, W -Z. Wu, An1ime1as1a1>c effect of Fucoidan-Sargassum against liver Cancer cell lnvadopodla formation vJa 1arge1ing in1egrin 11V1l3 and mediating ttV113/SrcJE2FI signaling J Cancer 10 (2019) 4777-4792,

(19] H.Y. Park. l.-W. Choi, G.-V Kim, B.W. Kim, W.-J. Kirn. Y.H. Choi, Fucotdan nduces Gt arre.- of ttle cell cycle in EJ hwnan bladder cancer cells lhroogh down, regulation of pRJI)lho!J)borylatlon, Rev. llr•s 25 (2015) 246-251.

(20] H. Y. Park. S.-H. **Park,** J.-W. Jeong, D. Yoon, M. H. Han, 0.-S. Lee, G. Chol. M.-J Yim, J.M. Lee, D.•H. Kim, G.•Y. Kim, l.,W. Choi, S. Kim, H.-S. Kim, H..J. Cha and Y. H. Choi, Induction of p53-lndependen1 apoptosls and GI cell cycle arrest by Fucoidan in HCTll6 hunum colorectal carcinoma cells. Mar. Drugs, 001:hnps :/ /doi.0tg/l 0.3390/md1506015-4.

(21) Z. Yao, H. Wu, S. Zhang, Y. Du, Enzym,otJc preparation of •-cartageenan ofiJo...,echarides and their antl-anglogenlc ac1iv,1y, Catb<Jhydr. Polym IOI (201◀) 359 367.

1221 M. Haijin, J. Xiaolu and G. Huashi, A -carragttMn Mrived oligosaccharide prepared by enzymatlc degrad•llon containing anti-tumor activil)'. Springer Scimtt and Business Media I.LC, 001:hnps·⌋ doi.O<g/10.1023 a.1025103530534.

1231 J. Li, K. Chen, S. Li, T. Liu, F Wang, Y Xia, J Lu, Y. Zhou, C. Guo, Pretreal- men! with Fucoldan from Fucus veslcul rus protected •gainsl ConA•L'lduced •cute liver in.Jury by inhibiting bo1h inlrlnste and umnsic •pop1osis, PloS One 11 (2016) e0152570.

(24) N. t:oonoo, **A.** Bhaw-Luximon, U. Jonas, 0. Jhurry, H. SchonhNT, Enhanced differentiation or human preosteoblas,s on electrospun blend fiber num or pol, dlo... none and anionic s,,J(ared polysaccharides, ACS Biomater Sci **Eng.** J (201 3447-3458.

1251 N. Goonoo, A. Fahrni, U. Jonas, F. Gim . l **A** Arsa, S Benard, H. S-honhert, A. Bhaw-Luximon, Improved multicellular response, b,omimelic minerHlizolio» angiogeiwsls, and reduced foreign body response of modified polydloxanone scaffolds for skeleial tissue regeneralion, ACS Appl. Mater. Interface< 11 (201 5834-5850.

(26) K. Adibkia, S. Hamedeyazdan Y. Javadzadeh, Drug release kineiia and phy"· cochemical characteristics of noating drug dellvery sys1ems Expert Op,n Drug DeliY 8 (2011) 891-903.

(27) C.G England, M.C. Miller, A. Kut1'1n, J O Trent, II B Frieboes, Release kt11e1,cs o(pad11axel and cisplalin from two and lhroe layered gold nanopart,cles, Eur J. Phartn Biopharm. 92 (2015) 120-12.9.

(28] R.J. Ruch, S.J. Cheng, J.E. Klaunig, Prevenllon of cylotoxicity and Inhibition *oi* inlercellulat comm.unic1uion by antioxidanl ca1«hlru isolated from Chinese grtt11 lea, Carcinogenesis 10 (1989> 1003-1008.

1291 N. Goonoo, F. Gimie, I. Ait•Arsa, C Cordorun, J Andnes, IJ. Jhurry. A. Bhaw-Lwc1mon Piezoelemlc core-shell PHBV 1>DX blend scaffolds for reduced s perfkoal wound contract,;,n and scMless tissue regeneration, lliomater S<1 9 (2021) 5259-527◀.

(30) S. McDougall, J Dallon, J Sherrall, P Mainl Fibroblast migration and collage deposition during dermal wound healing: mathematical modelling and clinic•I Implications, Philos. Transac1. A Math Phys. Eng. Sc,. 364 (2006) 1385-J 405.

(31) H.M. Rostam, P.M. Reynolds, M.R. Alexander, N Gadegaard, A. M. Ghaemmaghami, lmase based machine learning for iden1ifica1ion of macrophage subseu, Sci. Rep. 7 (2017) 3521

132) F.Y. McWhorter, T Wang. P. Nguyen, T Chung, W *F* Liu. Proc. Nall. Acad. 'i<1 U S. A 110 (2013) 17253-17258.

133) B. **Z.** Johnson, **A. W.** Stevenson, C. **M.** Peele, M. W. Fear and F. M. Wood, **Modulation** or **mattoJlha&e phenotype** by cell **shape.** *Bianitdicilles,* D01:10. 3390/ biOltlfllicines8050101.

(34) A.**A.** Al-Amiery, Y.K Al-Majedy, A.A.H. Kadhum, A.B Mohamad, Hydrage11 peroxide scavenging .telivil)' of novel coumarins synthes,zed using different approaches, P:OSOne JO (2015) c01J21? .

(35) J H. Naama, C.H. Alwan, M.R. Obayes, **A.A.** Al-Amiery, A.A. Al-Tem,mi, A.A. H. Kadhum, A.B. Mohamad, Curcum1noid5 as anllox,dants and theoreucal !ludy or subihty of curcumln ,somers in gaseous s1a1e, Res. Chem. Intertned. 39 (2013) 4 7-4059.

1361 A.F. llifney, M.A. Fawzy, KM. Abdel,Gawad, M. Gomaa, Industrial 01>1imi- zatlon of fucoidan cxtracuon from Sargassun1 sp. and its potential an ox1dan1and emulsifying acl,vil[es, Food llydrocoll 5-4 (2016) 77-88.

(371 II Qi, T. Zhao, Q Zhang, Z Li, Z. Zhao, R. Xing, An1iox1dan1 aclivily of difftr...,, molecul.lr wright sulfated polysacchartd"S from Ulva penUSA Kjellm (Chlorophyta) J Appl. Phycol. 17 (20051 527-SJ4.

(381 N Goonoo, R. Jce1ah, A. Bhaw,lu:umon, D Jhurry, Polydioxanone-b,,sed hi r.merials for i;ssue engineering and drug/gene delivery applicaUons, Eur. J. PhalTTl. Biopharm 97 (2015) 371-391.

[39) A. J. Gallagher, A Ni **Annaidh •nd** IC. Bruyere, Dynamic Tensde **Properties of Human** Skin. *2012 IRCOB/ Confrrenct*

(◀OJ C. Jac uemoud, K. Bruyere.Cam ,. M. Corel, Methodology to determine failure characteristics *oi* plan:1r soft timtes using a dtnamoc 1ens1le test. J Biomech. 40 (2007) 468-475.

[41) C.T Lim, E.P.S. Tan, S.V Ng, Effecl5 of crystaUlne morphology on lhe tensile properties of electrospun polymer nanofibcrs, Appl Phys Len 92 (2008) 141908.

(◀2) R.V. Philip, R.E. Harrison. A tenl pole lwisl on membrane ruffles, J Cell Biol 217 (2018) 3774-3775.

1◀3] W.G. Jiang, Focus on science--membrane rufning of cancer cells· a parameter of tumour cell mouluy **and** 1nvaS1on, European Journal of Surgical Oncology (EJSO) 21 (1995} 307-309.

(◀◀J 0 Akbik, M. Ghadirt W Chrzanowski, R. Rohanizadeh, Curcumin as **a** wound healing agenl, Life Set 116 (2014) 1-7,

145) G T Ge1hin S. Cowman, R.M Conroy, The impacl of Manuk• honey dres•ings on the surface pH of chronic wounds, lnl. Wound J 5 (2008) 18&-194.

(46] J M Reinke, H. Sorg, Wound repair and regener•lion, Eur Surg. Res. 49 (20121 35-43,

147) A.J Boutilier, S.F Els•w•. Macrophage polarizalton slates m the tumor Micro-environmen1. ln1 J Mol. <;c, 22 (13) (2021) 699&-7016.